The FEBS Journal

FEBS PRESS science publishing by scientists

Connecting color with assembly in the fluorescent B-phycoerythrin protein complex

Aneika C. Leney, Aline Tschanz and Albert J. R. Heck

Biomolecular Mass Spectrometry and Proteomics, Bijvoet Center for Biomolecular Research and Utrecht Institute for Pharmaceutical Sciences and Netherlands Proteomics Centre, Utrecht University, Utrecht, The Netherlands

Keywords
fluorescent probes; light-harvesting complex; native mass spectrometry; phycobiliproteins; phycoerythrin

Correspondence
A. C. Leney, Biomolecular Mass Spectrometry and Proteomics, Bijvoet Center for Biomolecular Research and Utrecht Institute for Pharmaceutical Sciences and Netherlands Proteomics Centre, Utrecht University, Padualaan 8, 3584 CH, Utrecht, The Netherlands
Fax: +31 030 253 6919
Tel: +31 030 253 6797
E-mail: a.c.leney@uu.nl

(Received 17 August 2017, revised 23 October 2017, accepted 13 November 2017)

doi:10.1111/febs.14331

Phycoerythrin is the major light-harvesting pigment protein in red algae and is nowadays widely used as a fluorescent probe in biotechnological applications such as flow cytometry and immunofluorescence microscopy. In addition, it has had substantial economic impact due to its potential as a natural food colorant. However, knowledge on the precise molecular composition of phycoerythrin is limited. Here, we use a combination of high-resolution native mass spectrometry (MS) and fluorescence spectroscopy to characterize the assembly properties of the B-phycoerythrin protein complex from *Porphyridium cruentum*. Our data highlight the stabilizing role of the γ subunit in the intact B-phycoerythrin protein complex. In addition, by native MS we monitor B-phycoerythrin (dis)assembly intermediates, providing insight into which species contribute to B-phycoerythrins color and the factors that give B-phycoerythrin its highly fluorescent properties. Together, the data provide significant insights into the structural properties of B-phycoerythrin which is beneficial for its use within the biotechnology industry.

Introduction

Currently there is substantial economic interest in microalgae due to their application as a natural source of compounds such as lipids, pigments, proteins, and polysaccharides [1,2]. Of these, natural pigments such as phycobiliproteins are of particular interest due to their biotechnological applications in food colorants, pharmaceuticals, and the cosmetic industry [3]. One prime example is phycocyanin, the most commonly used natural blue pigment in the food industry for products such as jelly and bubble gum [4]. Additionally, in biological and medical research applications, phycobiliproteins are increasingly utilized in flow cytometry, immunofluorescence activated cell sorting and *in vivo* imaging [5,6]. Their water soluble, highly fluorescent properties providing them with advantages over small organic dyes, whereby nonspecific binding is a common encounter [7].

Red algae contain three types of phycobiliproteins; allophycocyanins, phycocyanins and phycoerythrins, which together form a huge macromolecular complex termed the phycobilisome [8]. These phycobiliproteins absorb light over a wide range of wavelengths in the visible part of the spectrum, enabling the transfer of excitation energy to photosystems I and II. As such, visually, the phycoerythrins appear red, the phycocyanins purple-deep blue, and the allophycocyanins

Abbreviations
B-PE, B-phycoerythrin; ESI, electrospray ionization; MS, Mass spectrometry; PEB, phycoerythrobilin; PUB, phycourobilin.

The FEBS Journal **285** (2018) 178–187 © 2017 The Authors. *The FEBS Journal* published by John Wiley & Sons Ltd on behalf of Federation of European Biochemical Societies.

blue-green. The color of the phycobiliproteins being attributed to the presence of linear tetrapyrrole prosthetic groups, termed bilins that covalently link to specific cysteine residues on the protein subunits. Phycoerythrin, in particular, is considered the world's brightest natural fluorophore, being 10–20 times brighter than the best organic dyes [3]. Despite its biotechnological potential, fundamental knowledge on the molecular composition and structural arrangement of these multisubunit protein complexes is lacking. Moreover, it is only with increased knowledge on how these proteins function in the light-harvesting complex that phycobiliproteins can be specifically designed to harness their full potential.

B-Phycoerythrin (B-PE) from the unicellular red algae *Porphyridium cruentum* consists of multiple α and β subunits of 17 817 Da and 18 554 Da, respectively, and a third less well-characterized γ subunit with an apparent molecular mass of 30-33 kDa [9,10] (Fig. 1). The α subunit contains two covalently bound phycoerythrobilins (PEB) to cysteine residues 82 and 139, whereas the β subunit contains three PEBs, one bound to Cys82, one bound to Cys158, and the other one linked to both Cys50 and Cys61 [11]. In contrast, the γ subunit is predicted to contain four bilin subunits; two PEB and two phycourobilins (PUB) [10].

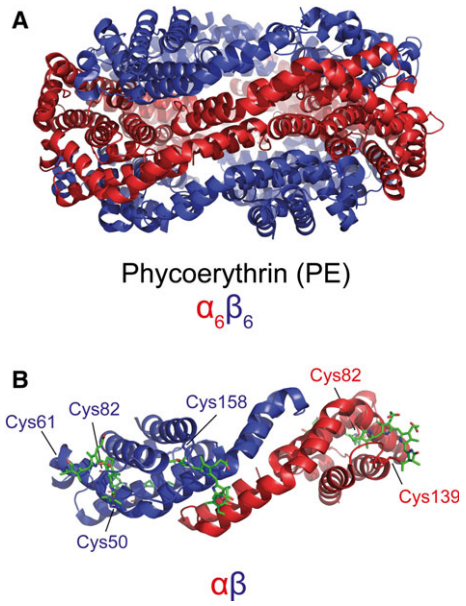

Fig. 1. Structure of the B-Phycoerythrin protein complex. (A) Side view of $\alpha_6\beta_6$ PE from *Phormidium rubidum* (PDB: 5AQD). (B) Side view of αβ dimer of B-PE (PDB:3V57). The bilin molecules on the α and β subunits are shown in green. The α and β subunits are colored red and blue, respectively. Note, although present during crystallization of B-PE, no structural information is available for the γ subunit.

Physiologically, B-PE is thought to reside as a large macromolecular complex composed of two $[(\alpha\beta)_2]_3$ hexamers and a single γ polypeptide [12]. The specific inter- and intramolecular interactions present within the complex are crucial for B-PE's role in light transmission. Yet, the specific nature of these interactions and how they contribute to fluorescence is largely unknown. Indeed, residual electron density in crystallography data has suggested the γ subunit is located in the center of the $[(\alpha\beta)_2]_3$ hexamers, but due to rotational averaging no structural data for γ has yet been obtained [12]. Moreover, it has been suggested that three or four different γ subunits may be present within the phycobilisome [11].

Efforts to date have been centered on utilizing techniques such as circular dichroism and UV-Vis spectroscopy combined with fluorescence spectroscopy to biophysically characterize B-PE [12–14]. However, these techniques lack high-resolution structural information, reporting only on the overall architecture of the protein–protein complexes in solution, and not on any unique, individual species that maybe present within the complex. Size exclusion chromatography has also been employed to characterize B-PE with limited success since the partially unfolded species at low and high pH interact strongly with the column material thus preventing quantitative information on all species in solution being obtained [13]. Thus, alternative methods are needed to monitor B-PE complex formation that would enable these B-PE complexes formed to be monitored as a function of fluorescence. Native mass spectrometry (MS), a technique in which proteins and their complexes are analyzed in their nondenatured state, is a fruitful, complementary method for characterizing the structure, stoichiometry and dynamics of protein complexes [15]. Soft ionization techniques, such as electrospray ionization, enable noncovalent complexes in solution to be transitioned into the gas phase for analysis, whereby each species can be uniquely separated on the m/z scale. Additionally, with the introduction of the Orbitrap mass analyzer with extended mass range, very high mass resolution on proteins and protein complexes can now be achieved [16,17] enabling even small post-translational modifications, such as glycosylation [18,19] and phosphorylation [20,21], to be uniquely resolved on proteins up to 150 kDa in size. Moreover, specific to photosynthetic complexes, native MS has recently offered new structural insights into the pigment-protein complex, FMO [22] and the phycobiliprotein, phycocyanin from *Thermosynechococcus vulcanus* [23].

Here, we characterize that B-PE from *P. cruentum* use a combination of native MS and fluorescence

spectroscopy. We show the importance of the γ subunit in stabilizing B-PE complex formation. Moreover, by monitoring B-PE assembly/disassembly, we show the factors that contribute to B-PE's color and how the bilin arrangement within these complexes contribute to B-PE's highly fluorescent nature.

Results

Native MS highlights role of γ subunit in stabilizing B-phycoerythrin

To determine the subunit stoichiometry of B-PE and thus which species contribute to its highly fluorescent properties, native MS was initially performed on B-PE at physiological pH. The predominant peaks in native mass spectrum consist of a narrow charge state distribution (33 + to 38 +) corresponding to an average molecular weight of 263.9 kDa (Fig. 2A, Table 1). This value is in the middle between the value reported from size exclusion chromatography (272 ± 5 kDa) [12] and the widely accepted molecular weight for B-PE of ~ 240 kDa [10,24], thus we attribute these peaks to the intact B-PE protein complex. Peaks were also observed at the lower m/z region corresponding to a protein complexes of 39 304 Da and 117 955 Da and at higher m/z corresponding to a complex of 528 kDa in size. These complexes were significantly lower in abundance in contrast with the intact 263.9 kDa B-PE protein complex suggesting that the 263.9 kDa B-PE protein complex is the most abundant complex in solution.

Tandem MS is commonly used to determine the subunit topology of large protein complexes [25,26].

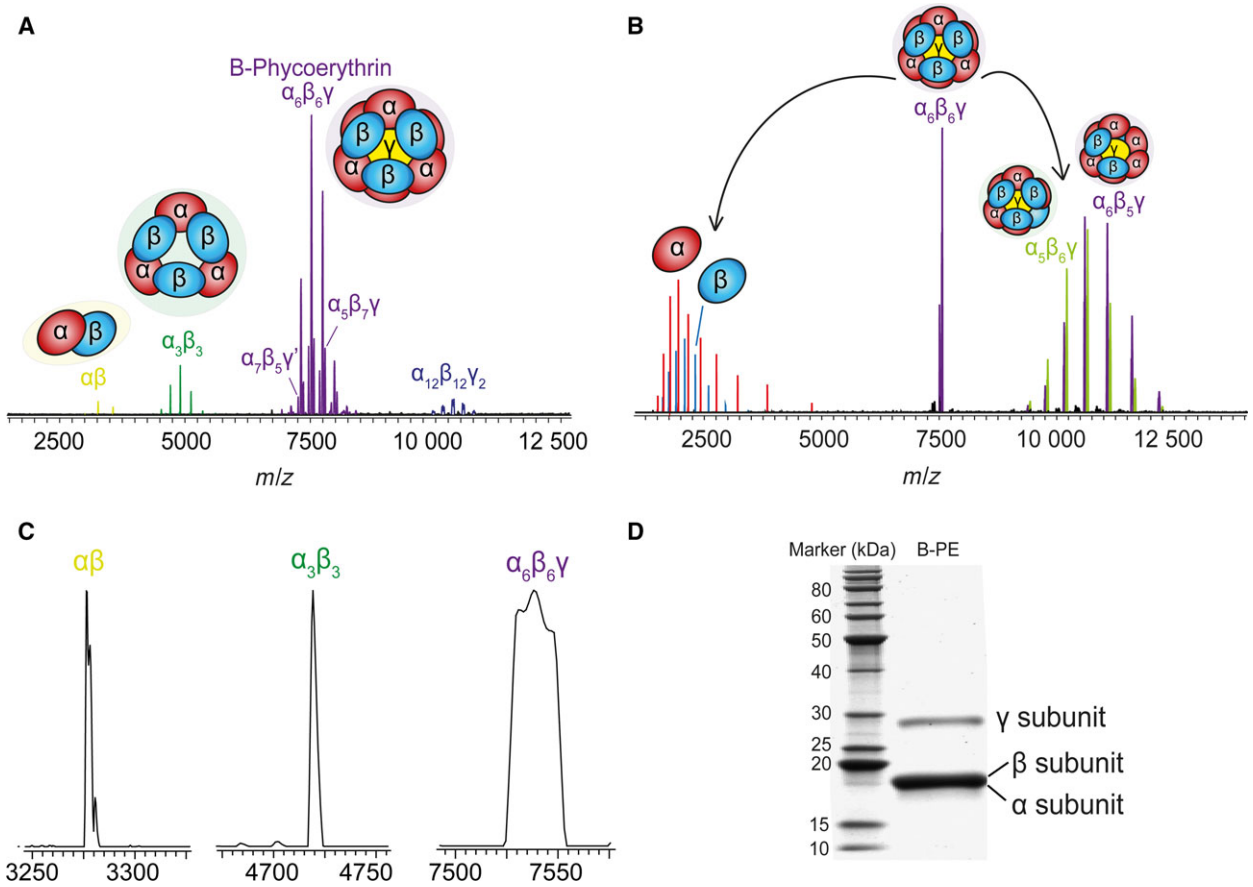

Fig. 2. Native MS of B-phycoerythrin reveals $\alpha_6\beta_6\gamma$ is the predominant species. (A) Native MS of B-PE at pH 7. The αβ, $\alpha_3\beta_3$, $\alpha_6\beta_6\gamma$, and $\alpha_{12}\beta_{12}\gamma_2$ complexes are shown in yellow, green, purple, and dark blue, respectively. (B) Tandem MS on $\alpha_6\beta_6\gamma$ complex shows release of α (red) and β (blue) monomers, and the γ subunit residing within the dissociated $\alpha_5\beta_6\gamma$ (green) and $\alpha_6\beta_5\gamma$ (purple) complexes. (C) Zoom in on $\alpha\beta^{12+}$, $\alpha_3\beta_3{}^{25+}$, and $\alpha_6\beta_6\gamma^{35+}$ peaks from native MS of B-PE at pH 7. The full width at half maximum (FWHM) of the $\alpha_6\beta_6\gamma$ complex (702 Da) is much broader when compared with the αβ (10 Da) and $\alpha_3\beta_3$ (58 Da) complexes, as a result of the heterogeneity in mass within the diverse set of gamma subunits. (D) SDS/PAGE analysis of B-PE showing presence of the α, β, and γ subunits.

Table 1. Experimentally determined molecular weights of observed proteins and protein complexes. The average molecular weights are reported for the proteins and protein complexes along with the monoisotopic molecular weight for the bilin subunit, phycoerythrobilin (PEB). Note, two species were observed for the β subunit corresponding to the presence one N-methyl asparagine on residue 72 alone [32] and in combination with another post-translational modification. Thus, since both β subunit isoforms were released from and thus reside within the intact B-PE complex, a molecular weight of 20 336 Da was used for the β subunit to calculate the expected molecular weights of all protein complexes. The standard deviation of the molecular weights calculated using all charge states is shown. For the γ subunit and $\alpha_6\beta_6\gamma$ complex, a range of molecular weights were reported since the peak width of the $\alpha_6\beta_6\gamma$ complex is broad (26 Th for 35 + charge state) compared with the expected peak width for a protein of comparable molecular weight (~ 6 Th) [27]. Thus, multiple γ species of differing molecular weights are likely present within the $\alpha_6\beta_6\gamma$ complex.

Protein Complex	Expected MW (Da)	Observed MW (Da)	Adducts
α	17805.0	18 977 ± 0.3	+1172 Da (= 2 × PEB)
β	18554.1	20 327 ± 0.3	+1773 Da (= 3 × PEB)
β_m		20 344 ± 0.6	
$\beta_{average}$		20 336	
$\gamma_{average}$	29 411–36 868[b]	27 312–28 192[a]	– ~ 5.4 kDa
αβ	39 304	39 304 ± 0.3	
$\alpha\beta_m$	39 321	39 325 ± 0.7	
$\alpha_2\beta_2$	78 625	78 635 ± 1.8	
$\alpha_3\beta_3$	117 938	117 955 ± 0.7	
$\alpha_4\beta_4$	157 251	157 292 ± 7.2	
$\alpha_6\beta_6\gamma$	265 235–272 692[b]	263 190–264 070	
PEB	586.3	-	

[a]denotes mass deduced from native MS of $\alpha_6\beta_6\gamma$ complex.
[b]denotes molecular weight based on predicted amino acid sequence for all PE-associated γ subunits [28].

Thus, to verify the subunit composition of the 263.9-kDa complex observed by native MS, ions corresponding to the 35 + charge state were isolated and subjected to gas phase dissociation (Fig. 2B). Two major charge state distributions were observed at low m/z values corresponding to protein molecular weights 18 977 Da and 20 327 Da. These correspond with the predicted molecular weights (based on amino acid sequence) of the α and β subunits of B-PE, whereby the α and β subunits have two and three PEB covalently attached, respectively (Table 1). In addition to the α and β subunit dissociation products, complementary fragmentation products were observed at higher m/z values consistent in molecular weight with the intact B-PE complex minus either one α or one β subunit (Fig. 2B, Table 1). Thus, the 263.9 kDa species was assigned to a $\alpha_6\beta_6$ complex with an additional 27.3–28.2 kDa species present which we attribute to the γ subunit. These $\alpha_6\beta_6\gamma$ peaks are significantly broader than what would be predicted for a homogeneous protein complex of similar size (Table 1) [27], thus consistent with previous observations [11], multiple γ isoforms are likely to reside within the complex. Interestingly, these γ subunits are much smaller than initially proposed based on SDS/PAGE analysis [10] and based on their predicted amino acid sequences (29.4–36.9 kDa) [28]. This suggests some degree of N- or C-terminal processing has occurred either pre- or post-B-PE assembly. Regardless of when this cleavage occurs, since the B-PE analyzed remains in its intact, functional state, these missing regions on γ are likely not necessary for B-PE complex formation.

Based on the α and β subunit molecular weights as determined by tandem MS experiments (Table 1), the low abundant 39-kDa and 118-kDa complexes in the native mass spectrum could be assigned to the αβ dimer and the $\alpha_3\beta_3$ complex, respectively (Fig. 2A). Interestingly, these complexes do not contain a γ subunit. In contrast, the $\alpha_6\beta_6$ complex is only observed with a γ subunit attached. Thus, we conclude that the γ subunit plays a critical role selectively in the formation and stabilization of the intact B-PE complex, likely, as previously suggested [29], residing within the two hexameric rings, linking the two $\alpha_3\beta_3$ complexes together.

Correlating the presence of αβ B-phycoerythrin intermediates with color

At physiological pH, B-PE is pink in color making it highly attractive for use in the food coloring and cosmetic industry (Fig. 3 and [13]). Upon lowering the pH, B-PE changes to a purple color (Fig. 3 and [13]), however, the structural reasons underlying this change are not known. Thus, next, we chose to monitor B-PE as a function of pH. Upon decreasing the pH from 8 to 6, no change in oligomeric species was observed by native MS (Fig. 3A). Consistent with this, no change in color (Fig. 3C) or fluorescence (Fig. 3B) was detected, suggesting that B-PE is fully stable over the pH range 6–8. At pH 5, a slight decrease in the fluorescence emission was observed (Fig. 3B). Differences were also observed in the native mass spectrum between pH 5 and pH 6–8. Specifically, at pH 5 the αβ dimer is the predominant species compared with the $\alpha_6\beta_6\gamma$ complex at pH 6–8. In addition, a $\alpha_2\beta_2$ complex becomes clearly visible at

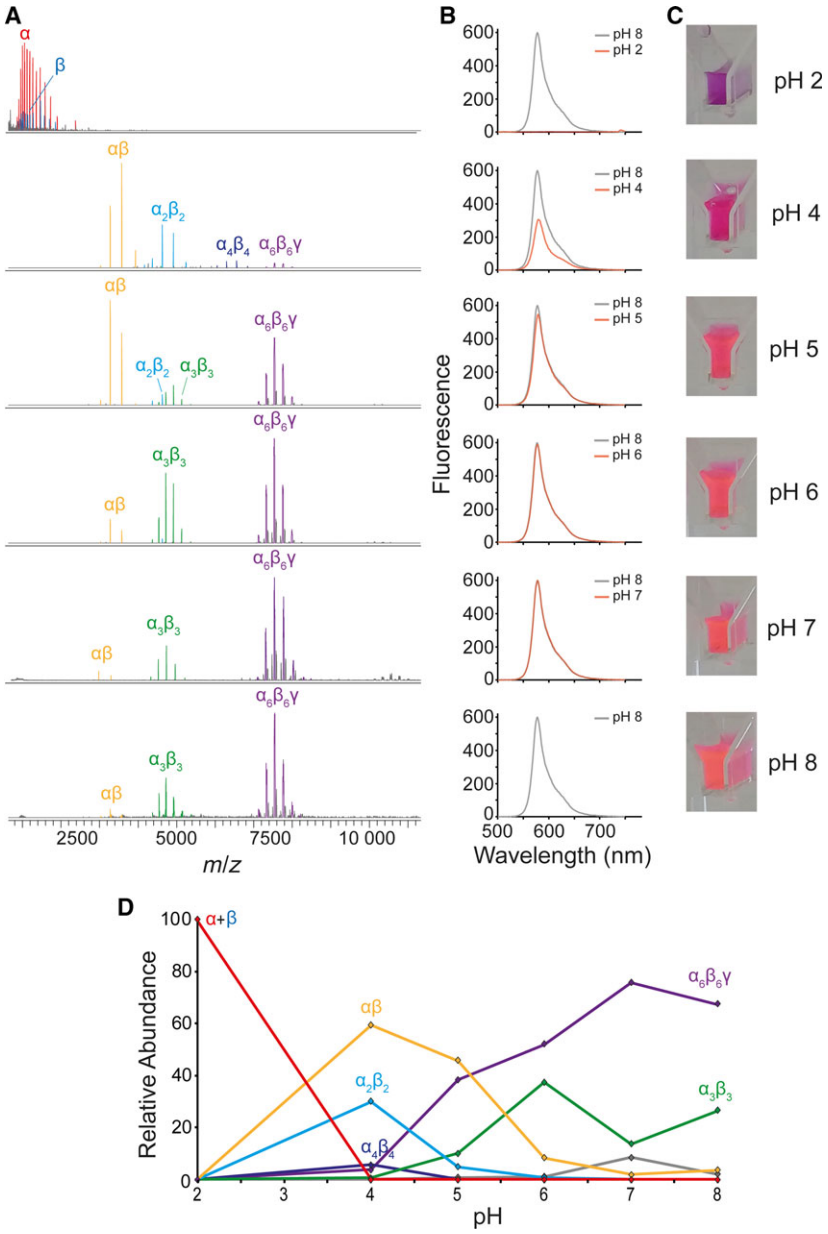

Fig. 3. B-Phycoerythrin dissociation and assembly can be regulated by pH. Native MS (A), fluorescence emission spectrum upon excitation at 498 nm (B), and color of B-PE (C) at pH 2, 4, 5, 6, 7, and 8. (D) Relative abundance of each species as determined by native MS as a function of pH. α, β, αβ, $\alpha_2\beta_2$, $\alpha_3\beta_3$, $\alpha_4\beta_4$, $\alpha_6\beta_6\gamma$, and $\alpha_{12}\beta_{12}\gamma_2$ complexes are shown in red, blue, yellow, blue, green, dark blue, purple, and gray, respectively. Note: various peaks corresponding to a diverse set of γ subunits are observed at pH 2, however, these are of very low intensity due to their heterogeneous nature.

pH 5. A more striking difference, however, is observed at pH 4. Here, B-PE changes color from pink to dark pink (Fig. 3C). This color change is consistent with a change in oligomeric species as detected by native MS (Fig. 3A). At pH 4, the $\alpha_6\beta_6\gamma$ complex decreases in intensity and αβ oligomers (αβ, $\alpha_2\beta_2$ and $\alpha_4\beta_4$) are observed. Interestingly, none of these αβ oligomers have a γ subunit attached suggesting that the γ subunit likely remains weakly attached within the $\alpha_6\beta_6\gamma$ complex and upon B-PE complex denaturation is rapidly released. B-PE complex dissociation at pH 4 corresponds with a decrease in fluorescence (Fig. 3B). However, it is important to note that the fluorescent properties of B-PE do not disappear completely at pH 4, suggesting although not as fluorescent as the $\alpha_6\beta_6\gamma$ complex, the αβ oligomers themselves likely possess fluorescent properties. At pH 2, no protein complexes were observed by native MS (Fig. 3A), no fluorescence was detected (Fig. 3B) and a color change was observed from pink (at pH 6–8) to purple (Fig. 3C). This fluorescence quenching mechanism observed at pH 2 is consistent with the lack of fluorescence detected upon B-PE denaturation in urea at neutral pH [30]. This strongly

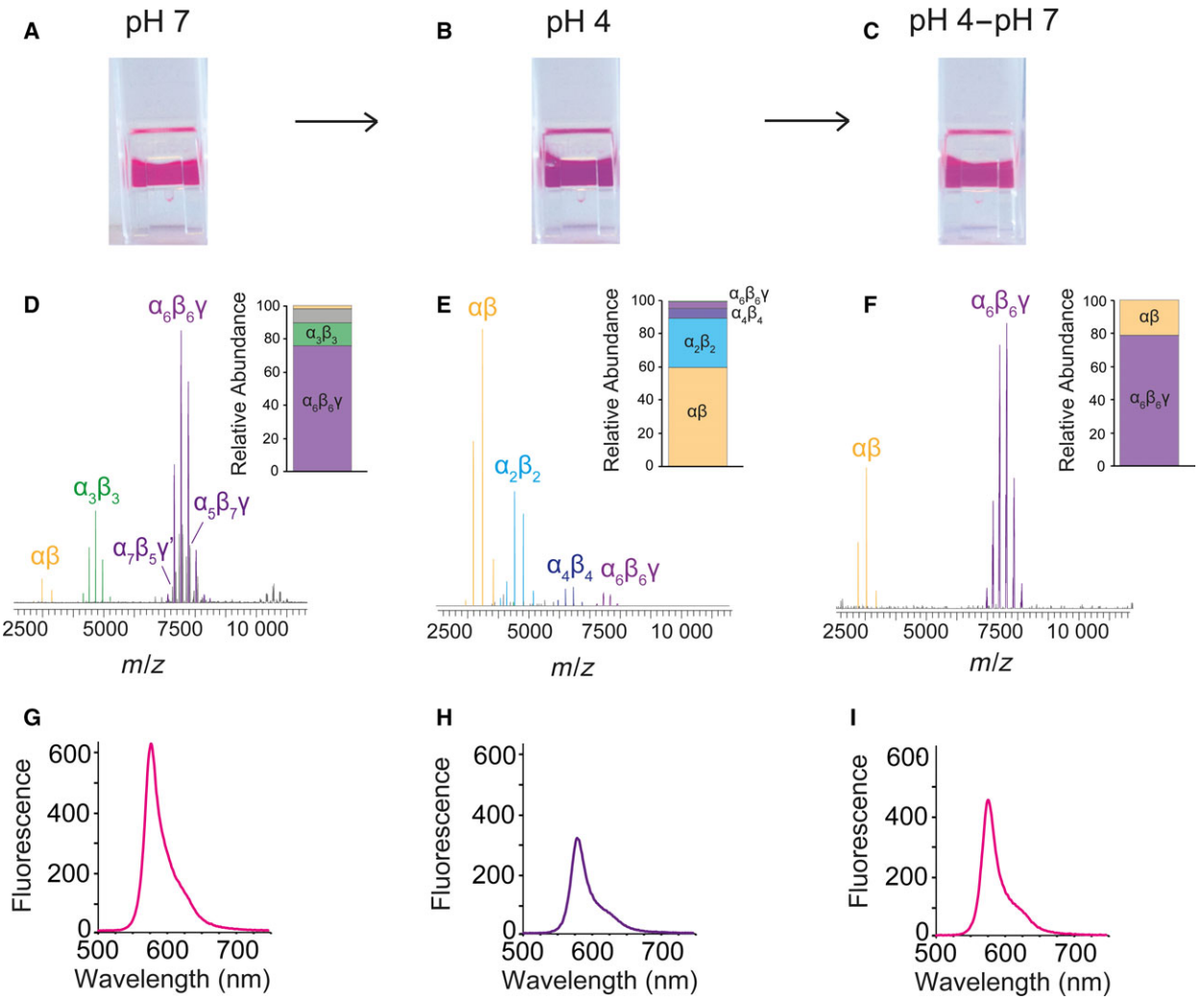

Fig. 4. B-Phycoerythrin dissociation/assembly is reversible. The color (A–C), relative abundance of each species as determined by native MS (D–F), and fluorescence emission spectra using an excitation wavelength of 498 nm (G–I) measured at pH 7 (A,D,G), pH 4 (B,E,H), and the pH 4 solution upon re-equilibration again to pH 7 (C,F,I). (For native MS data, see Fig. 3 legend for color scheme).

implies that complex formation is a prerequisite for B-PE pink color and highly fluorescent properties rather than the protonation of the chromophore. Indeed, this is consistent with previous studies whereby a loss of secondary structure was observed by circular dichroism at pH 2 [13].

The oligomeric species that predominate in solution upon decreasing the pH from 8 to 2 are shown in Fig. 3D. Upon decreasing pH, the γ subunit disappears first from the $\alpha_6\beta_6\gamma$ complex followed by the subsequent loss of $\alpha_2\beta_2$ tetramers until only the α and β monomers are present at pH 2. The presence of αβ oligomers at pH 4 suggests that, if the assembly process is reversible, the $\alpha_2\beta_2$ tetramer is likely the major building block during B-PE assembly.

Reversible assembly of B-PE

Due to the location of the phycobilisome on the thylakoid membranes, B-PE *in vivo* is constantly affected by environmental changes such as the pH gradient that is generated during photosynthesis. B-PE, therefore, needs to be able to adapt and respond to these conditions. PE assembly has proven to be reversible with another variant of phycoerythrin, R-PE which has different spectral properties to B-PE [31]. Thus, next, we chose to investigate whether this was also the case with B-PE. Upon decreasing the pH from 7 to 4 and back to 7 again, the initial color of B-PE could be restored (Fig. 4A–C). Although only an ensemble measurement, these data on color alone provides the first

evidence that the B-PE disassembly/assembly process is reversible between pH 4 and pH 7.

To probe B-PE reversibility in more detail, native MS was performed at pH 7 (Fig. 2A,4D), upon reducing the pH to 4 (Fig. 4E), and then again after increasing the pH back to 7 (Fig. 4F). At pH 4 the $\alpha_6\beta_6\gamma$ complex is almost completely disrupted with the $\alpha\beta$ dimer the most predominant species in the mass spectrum (Fig. 4E). However, upon re-equilibrating the pH back to 7, the $\alpha\beta$ oligomers observed at pH 4 disappear and the $\alpha_6\beta_6\gamma$ complex reforms (Fig. 4F) showing that B-PE complex formation is reversible. The transient nature of these $\alpha\beta$ oligomers implies, as we previously hypothesized, that the $\alpha_2\beta_2$ tetramer is the major building block during B-PE assembly. Upon comparison of the initial and refolded B-PE mass spectra, two minor differences can be noted. First, after reassembling the $\alpha_3\beta_3$ complex disappears. Second, the side peaks attributed to $\alpha_7\beta_5\gamma$ and $\alpha_5\beta_7\gamma$ complexes (Fig. 2A, Fig. 4D) are not present resulting in a 'cleaner' mass spectrum. The absence of these $\alpha_3\beta_3$, $\alpha_7\beta_5\gamma$ and $\alpha_5\beta_7\gamma$ complexes in the refolded B-PE spectrum suggests that these species are likely off-pathway and have formed as an artifact of protein complex extraction and purification.

The fluorescence properties of B-PE were next compared before and after reassembling (Fig. 4G–I). Consistent with the data obtained by native MS, B-PE fluorescence upon excitation at 498 nm decreased on reducing the pH to 4 (Fig. 4H) and increased again on restoring the pH back to 7 (Fig. 4I). This shows that not only the structural properties of B-PE can be restored but also B-PE can reassemble into its correct, functional state.

Discussion

B-phycoerythrin is one of the brightest natural fluorophores, yet the structural reasons behind its remarkable fluorescent properties are largely unknown. Here, we explored the relationship between the structure and function of B-PE using a combination of native MS, absorbance, and fluorescence spectroscopy. We show that at physiological pH, when B-PE exhibits its highest fluorescence, B-PE consists predominantly as a $\alpha_6\beta_6\gamma$ complex of 263.9 kDa in size (Fig. 2A, Fig. 3, Fig. 5). This complex, upon pH denaturation, dissociates by initial ejection of the γ subunit followed by sequential release of $\alpha_2\beta_2$ tetramers until at pH 2 only α, β, and γ monomers exist and no fluorescence is observed (Fig. 5, Fig. 3).

Our most interesting observation occurred at pH 4. Here, the $\alpha_6\beta_6\gamma$ complex is 95% dissociated yet the

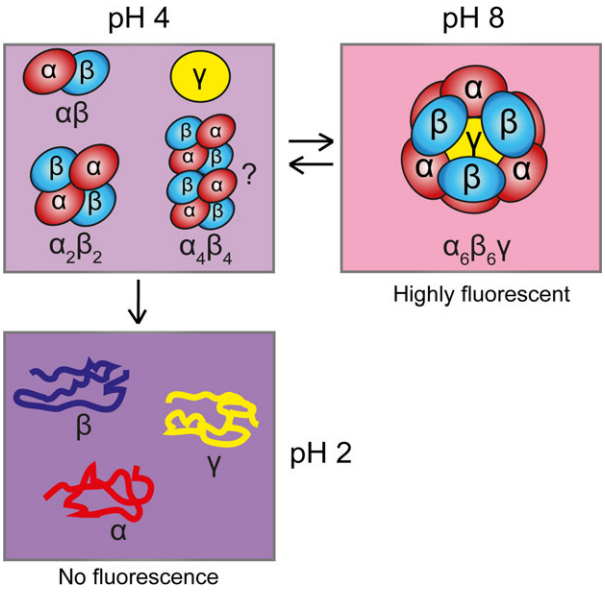

Fig. 5. Schematic of B-Phycoerythrin complex assembly. At physiological pH, B-PE consists predominantly as a highly fluorescent $\alpha_6\beta_6\gamma$ complex whereby γ resides at the center of the complex. B-PE dissociates at pH 4 into oligomers that consist of $\alpha\beta$ dimers. This dissociation correlates with a loss in B-PE fluorescence and is reversible. At pH 2, all B-PE complexes are disrupted with only the individual α, β, and γ subunits present in solution. The colors of the boxes represent the color of B-PE in solution at its relevant pH.

fluorescent properties of the B-PE solution are still maintained to a large extent (Fig. 3D, Fig. 4E,H). Thus, it is possible that the $\alpha\beta$ oligomers alone contribute to fluorescence and these fluorescent properties are simply enhanced when the γ subunit is present. In addition to enhancing fluorescence, we show the γ subunit plays an important role in stabilizing the intact $\alpha_6\beta_6\gamma$ complex, indeed, no $\alpha_6\beta_6$ complex was observed at any pH without the γ complex subunit present. Interestingly, previous work by Martínez-Rodríguez and coworkers showed no notable changes in fluorescence over a pH range of 4–10 from which it was hypothesized that B-PE is stable [13]. Indeed, consistent with their observations, we observed only a very small decrease in fluorescence between pH 4 and pH 8 (Fig. 3B, Fig. 4G,H). We show by native MS, however, significant structural rearrangements in, and partial disassembly of, the $\alpha_6\beta_6\gamma$ B-PE complex occurring at pH 4 (Fig. 3A, Fig. 4E). These changes are 'invisible' when monitoring B-PE by methods such as fluorescence spectroscopy, absorbance, or circular dichroism, revealing that B-PE is not that stable at pH 4. Thus, our results additionally highlight the advantages that native MS has in the monitoring of noncovalent photosynthetic protein complexes.

Finally, we show that B-PE assembles reversibly between pH 4 and pH 7 (Fig. 4). This enables B-PE to adapt *in vivo* to its changing environment. The knowledge that B-PE assembles reversibly is beneficial to the biotechnology industry, whereby a change in color reports accurately on the local environment surrounding B-PE. Additionally, since B-PEs color can be fine-tuned by pH alone, we expect the new-found properties of B-PE will help provide significant new insights into the utility of B-PE in biological and biomedical imaging applications.

Materials and methods

Native MS

B-phycoerythrin (B-PE) from *P. cruentum* was purchased from Thermo Fisher Scientific. For native MS analysis, B-PE was buffer exchanged into 200 mM ammonium acetate at pH 4, pH 5, pH 6, pH 7, and pH 8, and analyzed immediately using a Orbitrap EMR instrument (Thermo Fisher Scientific) operated in positive ion mode. B-PE was sprayed at a concentration of 5 μM using a nanoESI source and gold-coated borosilicate glass needles. A capillary voltage of 1.4 kV was applied and a source fragmentation of 0 eV. Native MS on B-PE was initially carried out on an LCT mass spectrometer (Waters) to optimize conditions. Based on these observations, the MS parameters were optimized on the Orbitrap EMR instrument to mirror the spectra obtained from the lower resolution LCT mass spectrometer. Consequently, in all cases, the source DC offset was set to 25 V, injection flatapole 8 V, interflatapole lens 7 V, bent flatapole DC 6 V, and transfer multiple DC 4 V. The trapping gas was set to 5. The HCD voltage and maximum injection time were set to zero and noise level to 2. All native MS was carried out at a resolution setting of 8750 and CsI used throughout for calibration. The accurate molecular weights of all proteoforms were calculated by averaging the molecular weights from a minimum of three differing charge states. For denaturing MS analysis, formic acid was added to B-phycoerythrin in 200 mM ammonium acetate pH 7 to a final pH of 2. The MS conditions used for denaturing MS (pH 2) were identical to those previously described except for the trapping gas which was lowered to zero to aid low m/z ion transmission. For all reassembly experiments, diluted B-PE in 200 mM ammonium acetate pH 4 was taken and concentrated to approximately 4 $mg{\cdot}mL^{-1}$ using an Amicon Ultra centrifugal filter with a 3 kDa MWCO. The B-PE complex was then reassembled by rapid dilution into 200 mM ammonium acetate pH 7. Note that the B-PE complex did not readily reassemble in ammonium acetate buffer after full denaturation of B-PE at pH 2.

MS/MS analysis

All tandem MS experiments were carried out on an Orbitrap Exactive Plus mass spectrometer (Thermo Fisher Scientific) modified for optimal transmission and detection of high m/z ions [16]. For effective transmission of large complexes, the injection flatapole was set to 7, interflatapole lens 6, bent flatapole DC 6, and transfer multiple DC 7. The most abundant charge state of the $\alpha_6\beta_6\gamma$ complex (35 +) was selected for HCD fragmentation using nitrogen as a collision gas. All MS spectra were processed using Xcalibur v2.2 (Thermo Fisher Scientific).

Fluorescence spectroscopy

Samples from native MS measurements were diluted to a concentration of 0.08 $mg{\cdot}mL^{-1}$ in 200 mM ammonium acetate at the relevant pH and fluorescence measurements taken after 10 min using a Cary Eclipse Fluorescence spectrophotometer (Agilent). The emission spectra shown were measured over the range 500–750 nm at an excitation wavelength of 498 nm. Emission spectra were also measured at an excitation wavelength of 540 nm and 565 nm. These spectra are consistent with those obtained by González-Ramírez *et al.* [13] demonstrating that the mass spectrometry buffer used (200 mM ammonium acetate) does not affect the fluorescent properties of B-PE. The excitation wavelengths were chosen based on the three characteristic peaks in the absorbance spectrum of B-PE at pH 7 [13]. A 1-cm path length cuvette was used and the temperature maintained at 21 °C throughout. Slit widths were set to 5 nm for both excitation and emission.

Acknowledgements

This work was supported by the Roadmap Initiative Proteins@Work (project number 184.032.201), funded by the Netherlands Organisation for Scientific Research (NWO).

Author contributions

ACL designed the study and performed the experiments and analyzed the data with help from AT. ACL and AJRH prepared the manuscript.

References

1 Stengel DB, Connan S & Popper ZA (2011) Algal chemodiversity and bioactivity: sources of natural variability and implications for commercial application. *Biotechnol Adv* **29**, 483–501.
2 Spolaore P, Joannis-Cassan C, Duran E & Isambert A (2006) Commercial applications of microalgae. *J Biosci Bioeng* **101**, 87–96.

3 Manirafasha E, Ndikubwimana T, Zeng X, Lu Y & Jing K (2016) Phycobiliprotein: potential microalgae derived pharmaceutical and biological reagent. *Biochem Eng J* **109**, 282–296.
4 Carle R & Schweiggert R (2016) Handbook on Natural Pigments in Food and Beverages: Industrial Applications for Improving Food Color. Woodhead Publishing, Duxford, UK.
5 Rodriguez EA, Tran GN, Gross LA, Crisp JL, Shu X, Lin JY & Tsien RY (2016) A far-red fluorescent protein evolved from a cyanobacterial phycobiliprotein. *Nat Methods* **13**, 763–769.
6 Sekar S & Chandramohan M (2008) Phycobiliproteins as a commodity: trends in applied research, patents and commercialization. *J Appl Phycol* **20**, 113–136.
7 Glazer AN (1994) Phycobiliproteins — a family of valuable, widely used fluorophores. *J Appl Phycol* **6**, 105–112.
8 Adir N (2005) Elucidation of the molecular structures of components of the phycobilisome: reconstructing a giant. *Photosynth Res* **85**, 15–32.
9 Swanson RV & Glazer AN (1990) Separation of phycobiliprotein subunits by reverse-phase high-pressure liquid chromatography. *Anal Biochem* **188**, 295–299.
10 Glazer AN & Hixson CS (1977) Subunit structure and chromophore composition of rhodophytan phycoerythrins. *Porphyridium cruentum* B-phycoerythrin and b-phycoerythrin. *J Biol Chem* **252**, 32–42.
11 Lundell DJ, Glazer AN, DeLange RJ & Brown DM (1984) Bilin attachment sites in the alpha and beta subunits of B-phycoerythrin. Amino acid sequence studies. *J Biol Chem* **259**, 5472–5480.
12 Camara-Artigas A, Bacarizo J, Andujar-Sanchez M, Ortiz-Salmeron E, Mesa-Valle C, Cuadri C, Martin-Garcia JM, Martinez-Rodriguez S, Mazzuca-Sobczuk T, Ibañez MJ *et al.* (2012) pH-dependent structural conformations of B-phycoerythrin from *Porphyridium cruentum*. *FEBS J* **279**, 3680–3691.
13 González-Ramírez E, Andújar-Sánchez M, Ortiz-Salmerón E, Bacarizo J, Cuadri C, Mazzuca-Sobczuk T, Ibáñez MJ, Cámara-Artigas A & Martínez-Rodríguez S (2014) Thermal and pH Stability of the B-Phycoerythrin from the Red Algae *Porphyridium cruentum*. *Food Biophys* **9**, 184–192.
14 Bermejo R, Talavera EM & Alvarez-Pez JM (2001) Chromatographic purification and characterization of B-phycoerythrin from *Porphyridium cruentum*. *J Chromatogr A* **917**, 135–145.
15 Leney AC & Heck AJR (2017) Native mass spectrometry: what is in the name? *J Am Soc Mass Spectrom* **28**, 5–13.
16 Rose RJ, Damoc E, Denisov E, Makarov A & Heck AJR (2012) High-sensitivity Orbitrap mass analysis of intact macromolecular assemblies. *Nat Methods* **9**, 1084–1086.
17 van de Waterbeemd M, Fort KL, Boll D, Reinhardt-Szyba M, Routh A, Makarov A & Heck AJR (2017) High-fidelity mass analysis unveils heterogeneity in intact ribosomal particles. *Nat Methods* **14**, 283–286.
18 Rosati S, Rose RJ, Thompson NJ, van Duijn E, Damoc E, Denisov E, Makarov A & Heck AJR (2012) Exploring an orbitrap analyzer for the characterization of intact antibodies by native mass spectrometry. *Angew Chem Int Ed* **51**, 12992–12996.
19 Leney AC, Rafie K, van Aalten DMF & Heck AJR (2017) Direct monitoring of protein O-GlcNAcylation by high-resolution native mass spectrometry. *ACS Chem Biol* **12**, 2078–2084.
20 Lössl P, Brunner AM, Liu F, Leney AC, Yamashita M, Scheltema RA & Heck AJR (2016) Deciphering the interplay among multisite phosphorylation, interaction dynamics, and conformational transitions in a tripartite protein system. *ACS Cent Sci* **2**, 445–455.
21 van de Waterbeemd M, Lössl P, Gautier V, Marino F, Yamashita M, Conti E, Scholten A & Heck AJR (2014) Simultaneous assessment of kinetic, site-specific, and structural aspects of enzymatic protein phosphorylation. *Angew Chem Int Ed* **53**, 9660–9664.
22 Wen J, Zhang H, Gross ML & Blankenship RE (2011) Native electrospray mass spectrometry reveals the nature and stoichiometry of pigments in the FMO photosynthetic antenna protein. *Biochemistry* **50**, 3502–3511.
23 Eisenberg I, Harris D, Levi-Kalisman Y, Yochelis S, Shemesh A, Ben-Nissan G, Sharon M, Raviv U, Adir N, Keren N *et al.* (2017) Concentration-based self-assembly of phycocyanin. *Photosynth Res* **134**, 39–49.
24 Beardslee T, Bogoev R, Bolz C, Rooney R & Updyke T (2007) Liquid protein markers for native gel electrophoresis.
25 Sobott F & Robinson CV (2002) Protein complexes gain momentum. *Curr Opin Struct Biol* **12**, 729–734.
26 Lössl P, van de Waterbeemd M & Heck AJ (2016) The diverse and expanding role of mass spectrometry in structural and molecular biology. *EMBO J* **35**, e201694818.
27 Lössl P, Snijder J & Heck AJR (2014) Boundaries of mass resolution in native mass spectrometry. *J Am Soc Mass Spectrom* **25**, 906–917.
28 Bhattacharya D, Price DC, Chan CX, Qiu H, Rose N, Ball S, Weber APM, Arias MC, Henrissat B, Coutinho PM *et al.* (2013) Genome of the red alga Porphyridium purpureum. *Nat Commun* **4**, 1941.
29 Ficner R & Huber R (1993) Refined crystal structure of phycoerythrin from *Porphyridium cruentum* at 0.23-nm resolution and localization of the gamma subunit. *Eur J Biochem* **218**, 103–106.
30 hEocha CÓ & Carra PÓ (1961) Spectral studies of denatured phycoerythrins1. *J Am Chem Soc* **83**, 1091–1093.

31 Liu L-N, Su H-N, Yan S-G, Shao S-M, Xie B-B, Chen X-L, Zhang X-Y, Zhou B-C & Zhang Y-Z (2009) Probing the pH sensitivity of R-phycoerythrin: investigations of active conformational and functional variation. *Biochim Biophys Acta* **1787**, 939–946.

32 Sidler W, Kumpf B, Suter F, Klotz AV, Glazer AN & Zuber H (1989) The complete amino-acid sequence of the alpha and beta subunits of B-phycoerythrin from the rhodophytan alga *Porphyridium cruentum*. *Biol Chem Hoppe Seyler* **370**, 115–124.